MADE EASY
India's Best Institute for IES, GATE & PSUs

Detailed Solutions

ESE-2024 Mains Test Series

Mechanical Engineering Test No : 6

Section A : Renewable Sources of Energy + Industrial and Maintenance Engg. [All Topics]
Section B : Production Engineering & Material Science-1 [Part Syllabus]
Theory of Machines-2 [Part Syllabus]

Section A

1. (a)

The actual value of cell output voltage, V attained on load is less than E. The difference between actual and theoretical voltage is known as polarisation, V_p The effect of polarisation is to reduce the voltage and thereby efficiency of the cell from its maximum value. All the losses in the fuel cell may be included under voltage efficiency, which may be expressed as

$$\eta = \frac{\text{on load voltage}}{\text{theoretical open circuit voltage (emf)}} = \frac{V}{E}$$

The VI characteristic of a fuel cell is shown in figure. Voltage regulation is poor for small and large values of output current. Therefore, in practice the operating point is fixed in the range BC of the characteristics where voltage regulation is best and the output voltage is roughly around 0.6–0.8 V.

At no load, the terminal voltage is equal to the theoretical open-circuit voltage. As the cell is loaded (current is supplied to load), voltage and hence efficiency drops significantly. The departure of output voltage from ideal emf is mainly due to the following reasons.

(i) Activation Polarisation (Chemical Polarisation) : This is related to activation energy barrier for the electron transfer process at the electrode. Certain minimum activation energy is required to be supplied so that sufficient number of electrons is emitted. At low current densities significant numbers of electrons are not emitted. This

energy is supplied by the output of the cell, resulting in potential loss. It can be reduced by an effective electrochemical catalyst and also by increasing the operating temperature.

(ii) Resistance Polarisation : At larger current, there is additional contribution from internal electrical resistance of the cell. The internal resistance is composed mainly of resistance of bulk electrolyte and interface contact resistance between electrode and electrolyte. The resistance polarisation can be reduced by (a) using more concentrated (i.e., high conductivity) electrolyte, (b) increasing the operating temperature, and (c) using proper shape and spacing of electrolyte to reduce the contact resistance.

(iii) Concentration Polarisation : This type of polarisation tends to limit the current drawn from the cell. This is related to mass transport within the cell and may further be subdivided into two parts.

(a) Electrolyte Polarisation : It is due to slow diffusion in the electrolyte causing change in concentration at the electrode. This effect can be reduced by increasing the electrolyte concentration or by stirring/circulating the electrolyte.

(b) Gas-side Polarisation : It is caused due to slow diffusion of reactants through porous electrode to the site of reaction or slow diffusion of product away from the reaction site. Increasing the operating temperature also reduces this effect.

As observed in the above discussion, all the losses in the fuel cell are reduced as operating temperature is increased. Therefore, in practice, a fuel cell is usually operated at the higher end of its operating temperature range.

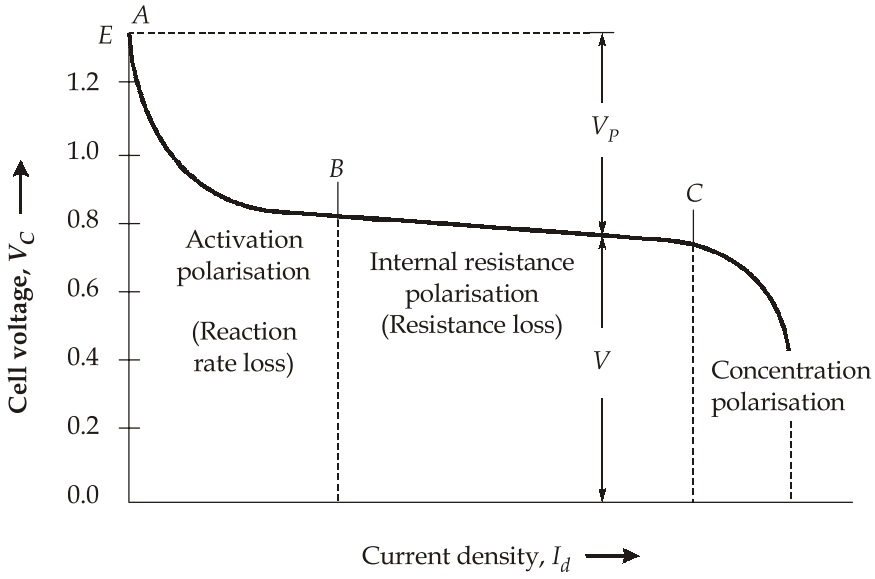

VI characteristic of fuel cell

1. (b)

Present plant capacity, n = 3200 units

Profit, $P = (s - v)n - F$

$$P = \left(\frac{10500000}{3200} - 4200\right) \times 3200 - 4000000 = ₹-6940000$$

Full capacity of the plant, $n' = \frac{3200}{0.8} = 4000$ units

Fixed cost, F' = ₹4800000/-

Variable cost, v' = 4200 – 800 = 3400/unit

$\therefore$ Profit, $P' = (s - v')n' - F$

$$= \left(\frac{10500000}{3200} - 3400\right) \times 4000 - 4800000$$

P' = ₹ –5275000

Thus the proposal is economical since it reduces the loss by ₹1665000/-.

1. (c)

n = 120; t = 1 hr; T = 15000 hours

The probability of failure, $P_{f_1} = \frac{n \cdot t}{T} = \frac{120 \times 1}{15000} = 8 \times 10^{-3}$ **Ans. (i)**

The group redundancy case,

The probability of failure if the elements are grouped as a set

$$P_{f_2} = N \cdot n \cdot \left(\frac{t}{T}\right)^2$$

$$= 120 \times 10 \times \left(\frac{1}{15000}\right)^2 \quad \text{[where } N = 10 \text{ elements]}$$

$= 5.33 \times 10^{-6}$ **Ans. (ii)**

The reliability improvement factor,

$$\text{RIF} = \frac{\text{Probability of failure before improvement}}{\text{Probability of failure after improvement}}$$

$$= \frac{P_{f_1}}{P_{f_2}} = \frac{8 \times 10^{-3}}{5.33 \times 10^{-6}} = 1500.94$$ **Ans.(iii)**

1. (d)

Sunshine Recorder : A sunshine recorder is a device used to measure the "hours of bright sunshine in a day".

The description of a sunshine recorder is given below:

Construction: It consist of a "glass-sphere" installed in a section of "spherical metal bowl" having grooves for holding a "recorder card strip" and the glass sphere.

Working: The glass-sphere, which acts as a convex lens, focusses the sun's rays/beams to a point on the card strip held in a groove in the spherical bowl mounted concentrically with the sphere.

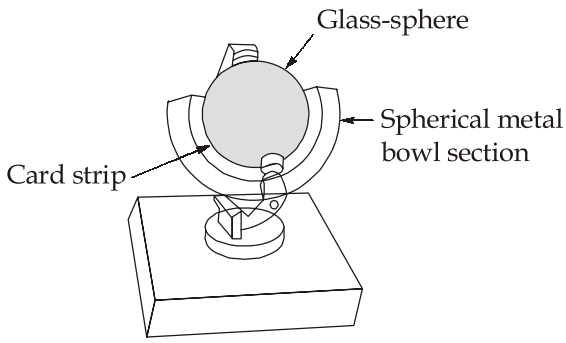

Sunshine recorder

Whenever there is a bright sunshine, the image formed is intense enough to burn a spot on the card strip. Through the day, the sun moves across the sky, the image moves along the strip. Thus a burnt space whose length is proportional to the duration of sunshine is obtained on the strip.

$$\phi\,(\text{Mumbai}) = 19.12°;$$

$$n = 309 \text{ [for } 5^{\text{th}} \text{ of November]};$$

$$\text{Hour angle at noon, } \omega = 0$$

$$\text{The declination angle, } \delta = 23.45 \times \sin\left(\frac{360° \times n}{365}\right)$$

$$= 23.45 \times \sin\left(\frac{360° \times 309}{365}\right) = -19.26°$$

The incidence angle is given by,

$$\cos\theta = \sin\phi \cdot \sin\delta + \cos\phi \cdot \cos\delta \cdot \cos\omega$$

$$\cos\theta = \sin(19.12°) \cdot \sin(-19.26°) + \cos(19.12°) \cdot \cos(-19.26°) \cdot \cos(0°)$$

$$\cos\theta = 0.7839$$

$$\theta = 38.38°$$

1. (e)

The condition monitoring, also known as dynamic predictive maintenance is composed of several functional aspects on which the maintenance is carried out. However, there are four important schematic and functional steps observed in any implementation of condition monitoring activity.

(a) Detection

(b) Diagnosis

(c) Prognosis (or Prediction)

(d) Programme (or Plan)

(a) **Detection :** This pillar of DPM details 'when' of the developing fault has just arisen. This focuses to answer the following 'when' questions.

- When might the fault have started?
- When (or how early) is the fault noticed?
- When does this fault result in a disaster if left unattended?

(b) **Diagnosis:** Diagnosis concentrates on knowing 'what' of the origin of the fault so that spare parts can be ordered.

- What is origin of the fault?
- At what stage is the fault now?
- What is the growth rate of the fault?
- What are the components or parts that have been suffering from this fault?

(c) **Prognosis:** This pinpoints what could happen if the fault is left unattended, i.e., the forecast of after effects. It is to estimate the severity of the fault, possibility, and/or frequency recurrence of the fault and operational problems. This function puts the effort to answer the following queries.

- What is the severity of the fault?
- What could be the results of the fault?
- What could be the production loss?
- What is cost of the fault in terms of hours of production and maintenance or repair?
- What are the side effects?
- What is the trend of the failure? (progressive/constant/retrogressive)
- What is the lead time?

(d) **Programme:** This function is concerned with preparation of schedule to enable the repair, schedule to be planned. This function attempts to reply the following type of questions.

- When should the equipment be taken for maintenance or repair?
- What maintenance policy should be adopted?
- When should the restoring action start and likely time when it can be finished?
- Who will maintain or repair so as to restore the condition?
- What is the action plan?

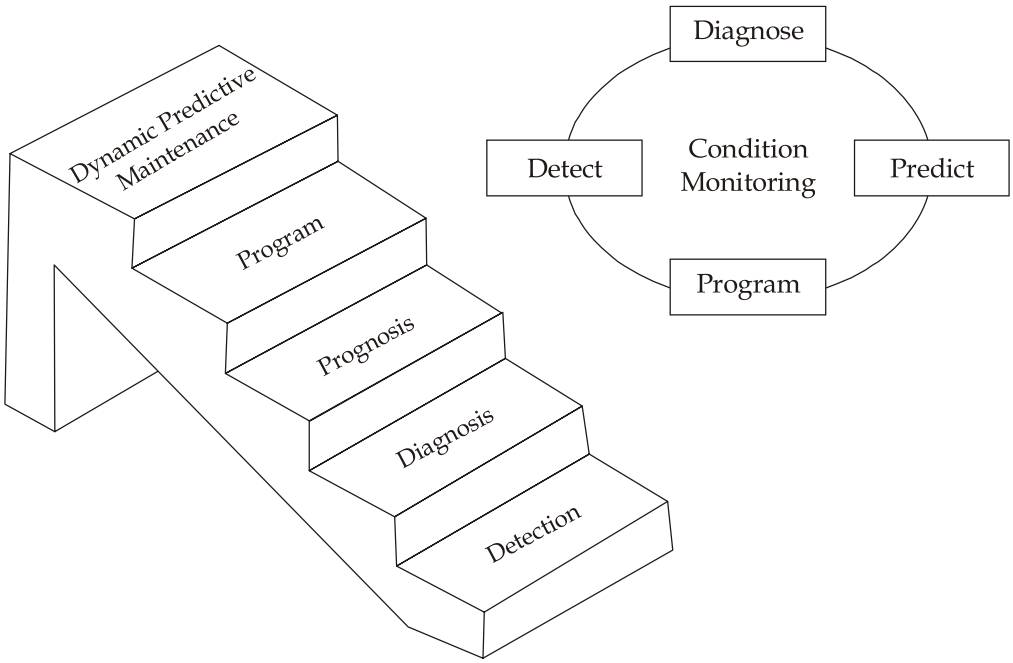

Figure : Four steps to reach dynamic predictive/condition-based maintenance

2. (a)

Figure below shows the two DC-DC converters connected in parallel. One of these is fed from PV, while the other is fed from fuel cell. Besides reliability, the other advantage of the system is the easy synchronization as compared to the synchronization of the two AC sources. Even if the insolation varies, the output power supplied to the load can be maintained by drawing the deficit power from the fuel cell. The DC-DC converter is operated to obtain the maximum power from PV array.

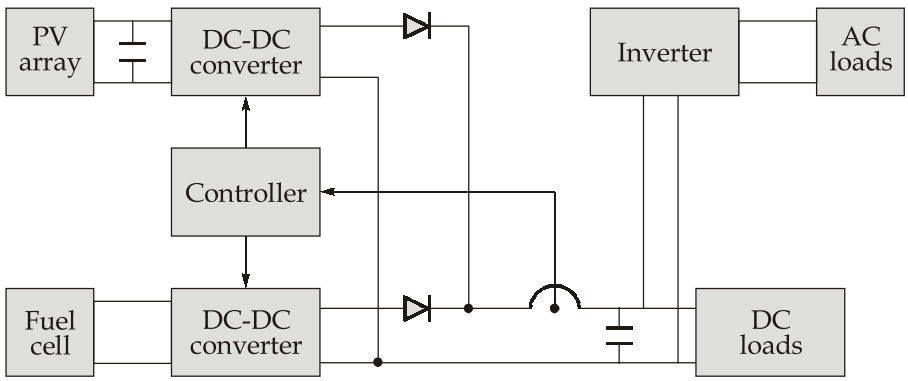

PV-fuel cell hybrid system

Some of the issues and problems related to the hybrid PV systems are as follows:

1. Most of the hybrid-PV systems require battery, which not only increases the cost, but also requires continuous monitoring. In addition, the battery life is limited to a few years (typically 3-4 years). It is reported that the battery lifetime should increase to around 10 years for the economic use in hybrid PV systems.
2. The other significant issue raised by the hybrid PV system is the load sharing between the different sources employed for power generation. The optimum power dispatch and the determination of cost per unit generation are not easy as it involves the sources that are dependent on weather.
3. The reliability of power can be ensured by incorporating weather independent sources like fuel cell. But fuel cell technology still requires some research related to the storing of hydrogen.
4. As the power generation from different sources of the hybrid-PV systems is comparable, a sudden change in the output power from any of the sources can affect the system stability significantly. Similar scenario results when there is a sudden change in the load. This presents a challenging task to design a fast and accurate control scheme to ensure system stability in such conditions.
5. Load sharing in the hybrid PV system is often not linked to the capacity or ratings of the sources. In fact, it is decided on several factors like the reliability of the source, economy of use, switching required between the sources, availability of the fuel, etc. As a result, a individual sources of the hybrid systems may operate at a point that is far from the point, which gives the most efficient operation. It is desired to evaluate the schemes, which, in spite of certain constraints, increase the efficiency to as high a level as possible.

2. (b)

Let x_1 and x_2 designated the number of Grade *A* and Grade *B* inspectors, respectively.

Hourly costs of each Grade *A* and Grade *B* inspectors are given by:

$$\text{Grade A inspector} = ₹(40 + 20 \times 0.02 \times 25)$$
$$= ₹50$$
$$\text{Grade B inspector} = ₹(25 + 20 \times 0.05 \times 20)$$
$$= ₹45$$

Using the given information, the appropriate linear programming problem is

$$\text{Minimize} \quad z = 8 \times 50x_1 + 8 \times 45x_2$$
$$\text{or} \quad z = 400x_1 + 360x_2$$

Subject to the constraints:

$$8 \times 25x_1 + 8 \times 20x_2 \geq 2000$$

or

$$5x_1 + 4x_2 \geq 50 \quad \text{(Number of pieces)}$$

$$x_1 \leq 8,\ x_2 \leq 10 \quad \text{(Number of inspectors)}$$

$$x_1 \geq 0,\ x_2 \geq 0 \quad \text{(Non-negative restrictions)}$$

Using graphical method, the feasible area obtained is shown below:

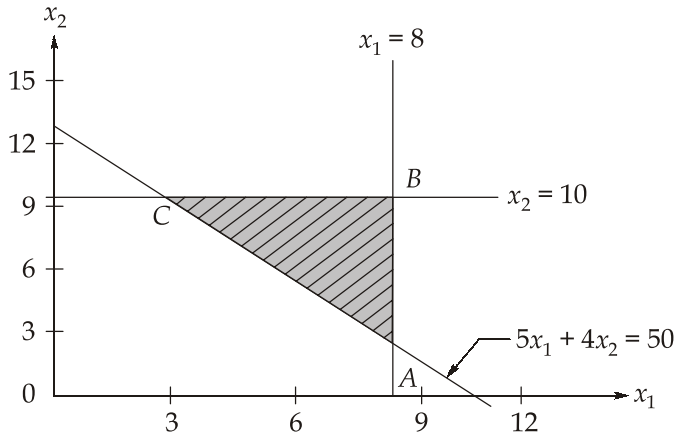

The coordinates of the extreme points are:

$$A = (8, 2.5),\ B = (8, 10) \text{ and } C(2, 10)$$

The z-value corresponding to the extreme points are:

Extreme point	(x_1, x_2)	$z = 400\,x_1 + 360\,x_2$
A	(8, 2.5)	4100 ← Minimum
B	(8, 10)	6800
C	(2, 10)	4400

Hence, the optimum solution is:

$$x_1 = 8;\ x_2 = 2.5 \simeq 3;\ z_{\min} = 4100$$

Thus, 8 Grade *A* inspectors and 3 grade *B* inspectors should be assigned to have ₹4100 as the total minimum inspection cost.

2. (c)

A loss in a solar cell refers to loss of photon energy (partial or full) which, due to some reason, is not able to deliver an electron out of a solar cell. This loss could be due to the fundamental reason, reason (limited by material properties) or it could be due to the technological reason (limited by cell processing capabilities). There are several ways in which photon energy loss could occur.

Loss of low energy photons: The photons having energy less than the band gap energy do not get absorbed in the material and, therefore, do not contribute to the generation of electron- pairs. This is referred as transmission loss, and is almost equal to 23% for a single junction solar cell.

Loss due to excess energy of photons: In an ideal case only, photon of energy equal to the band gap energy is required to excite an electron from valence band to conduction. When the photon energy E is higher than the band gap energy E_g, the excess energy = $E - E$, is given off as a heat to the material. This loss is referred as the thermalization loss. For a single junction solar cell, this is equal to about 33%.

Voltage loss: The voltage corresponding to the band gap of a material is obtained by dividing the band gap (potential energy) by charge, i.e., E_g/q. This is referred as the band gap voltage. The actual voltage obtained from a solar cell is V_{oc}. This happens due to the unavoidable intrinsic Auger recombination. The ratio of $V_o/E_g/q$ lies in the range of 0.65 to 0.72.

Fill factor loss: The I-V curve of ideal solar cell is square (i.e., $FF = 1$), but in reality, the cell I-V curve is given by the exponential behaviour. In the best case, the FF could be 0.89. This type of loss arises from the parasitic resistance (series and shunt resistance) of the cell.

The losses due to the technological reasons are as follows:

Loss by reflection: A part of incident photons is reflected from the cell surface. The reflection can be minimized by using anti-reflective coating and surface texturing.

Loss due to incomplete absorption: It refers to the loss of photons which have enough energy (i.e., > E_g) to get absorbed in the solar cell, but do not get absorbed in the cell due to limited solar cell thickness. The incomplete absorption is becoming important in the current scenario as the thickness of the cell (both wafer based and thin film) is being reduced in order to save the active material for cost reduction purpose. This type of loss can be minimized by having appropriate light trapping schemes.

Loss due to metal coverage: In wafer-based solar cell, the contact to the front side of the cell (from where light enters) is made in the form of finger and busbar. This metal contact shadows some light which can be up to 10%. Several approaches have been adopted to minimize this loss which include one-side contacted cell, buried-contact solar cell or transparent contact as used in thin film solar cells.

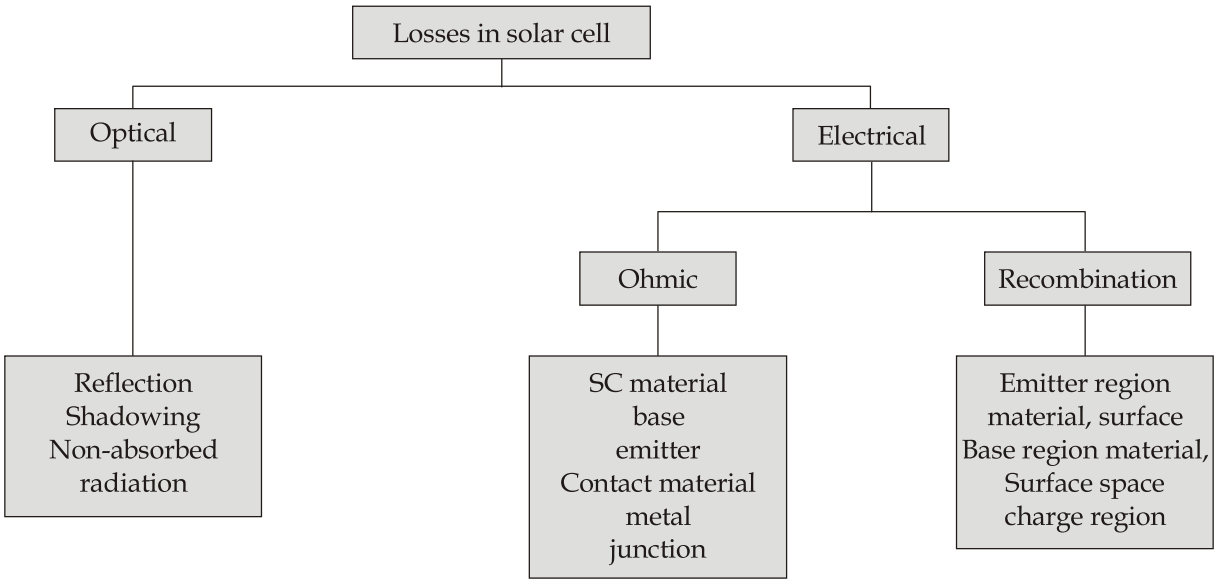

Categorization of loss mechanisms in solar cell arising from technological limitations

Recombination losses: Not all the generated electron-hole pairs contribute to the solar cell current and voltage due to recombination. The recombination could occur in the bulk of material or at the surfaces. This type of recombination can be minimized by appropriate surface and bulk passivation techniques.

The optical loss is referred to as the loss of photons which may result in the generation of electron-hole pairs. And the electrical loss is referred to as the loss of photons, which are absorbed in solar cell, but do not contribute to the cell output power due to either recombination or ohmic losses.

The optical losses can be reduced by the following design:

- Putting anti-reflection coating on the solar cell surface;
- Texturing front surface to reduce the reflection;
- Minimizing the front metal contact coverage area to reduce contact shading; and
- Making solar cell thicker to increase absorption of low energy photons.

3. (a)

Subtracting the smallest element of each row from every element of that row and then subtracting the smallest element of each column from every element of that column, we get the reduced distance table:

	a	*b*	*c*	*d*	*e*
A	2	2	0	4	0
B	6	4	0	10	2
C	0	1	0	1	2
D	2	4	0	4	2
E	2	0	0	0	2

In the reduced distance table, we make assignment in rows and columns having single zeros and cross off, all other zeros in those rows and column, where assignments have been made. Draw the minimum number of lines to cover all the zeros.

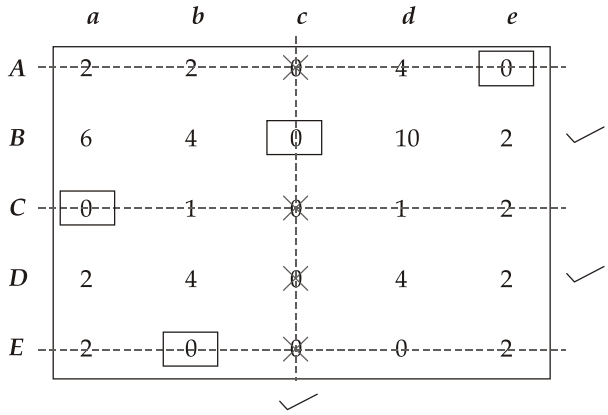

Modify the above table by subtracting the smallest element not covered by linear from all the uncovered elements and the same at the intersection elements of the lines. The modified table so obtain is shown below:

	a	*b*	*c*	*d*	*e*
A	2	2	2	4	0
B	4	2	0	8	0
C	0	1	2	1	2
D	0	2	0	2	0
E	2	0	2	0	2

Repeat the above procedure to find the new assignment, we get

	a	b	c	d	e	
A	2	2	2	4	0	✓
B	4	2	0	8	~~0~~	✓
C	0	1	2	1	2	✓
D	~~0~~	2	~~0~~	2	~~0~~	✓
E	2	0	~~2~~	~~0~~	2	
	✓	✓			✓	

Clearly the assignment shown in above table is also not optimum. To get the next solution, we draw the minimum number of horizontal and vertical lines to cover all the zeros. Subtracting the smallest uncovered element from all uncovered elements and adding the same to the intersection element of two lines gives us the table shown below.

	a	b	c	d	e
A	2	1	2	3	0
B	4	1	0	7	~~0~~
C	~~0~~	0	2	0	2
D	0	1	~~0~~	1	~~0~~
E	3	~~0~~	3	0	3

Since the number of assignments is equal to the order of the given matrix, an optimum solution is attained. Since, both the rows 'C' and 'E' have two zeros, the arbitrary selection of a cell in any of these two rows will give us an alternative solution having the same total distance.

Total minimum distance = 80 + 66 + 66 + 112 + 75

= 399 km **Ans.**

Optimum assignments:

$A \rightarrow$ e; $B \rightarrow$ c; $C \rightarrow$ b; $D \rightarrow$ a; $E \rightarrow d$

or

$A \rightarrow$ e; $B \rightarrow$ c; $C \rightarrow$ d; $D \rightarrow$ a; $E \rightarrow d$

3. (b) (i)

SN	Feature	Floating drum	Fixed dome
1.	Cost	More (due to steel drum)	Less
2.	Corrosion	Yes (likely in steel drum)	No
3.	Maintenance	More • drum requires painting, once or twice a year) • flexible gas pipe requires replacement	Less • no steel part is used • gas pipe is a fixed GI pipe
4.	Thermal insulation	Bad (heat loss due to steel drum)	Good (temperature will be constant due to complete under-ground construction)
5.	Scum troubles	By rotation of drum (no stirrer required)	More likely
6.	Gas production per unit volume of digester	High (due to bifurcation, both acid and methane formers find better environment for growth)	Low
7.	Scum braking	By rotation of drum (no stirrer required)	External stirrer is required
8.	Leakage	Less likely	More likely
9.	Danger of mixing with oxygen due to leakage, cracks	No	More likely
10.	Gas pressure	Constant	Variable
11.	Masonry work manship	Average skill	Specialized, skilled masonry work required

3. (b) (ii)

Based on the feedstocks, biofuels are categorized as first-generation, second- generation, third-generation, and fourth-generation biofuels as shown in figure.

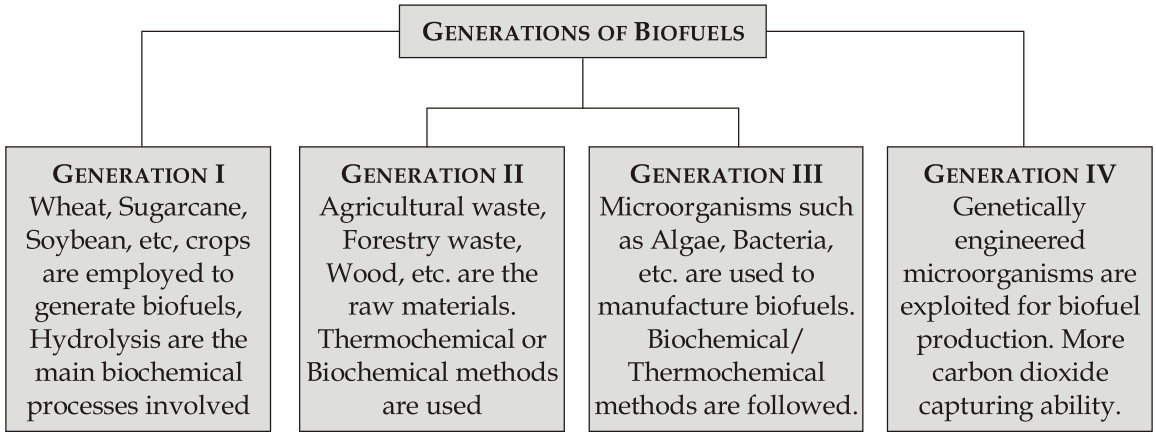

Biofuels derived from crop plants such as jatropha, almond, barley, camelina, coconut, copra, fish oil, groundnut, laurel, oat, poppy seed, okra seed, rice bran, sesame, sunflower, sorghum, wheat soybean, rapeseed, and karanja are termed as first-generation feedstocks. Biofuel production from such feedstocks faces criticism due to the food versus fuel dilemma. The value of food waste has not been paid much attention due to the lack of application policies and suitable management laws. Materials are also used to produce biofuels, known as second-generation feedstocks. However, these feedstocks do not have a stable supply to fulfill future energy needs. Alternatively, microorganisms, called third-generation feedstocks, can be used. A wide variety of microorganisms have been identified which serve as a sink for CO2 and produce biofuel. Genetically engineered microorganisms and algae constitute fourth-generation feedstock material. Optimization of processes for effective and efficient biomass conversion for all generations of biofuels and for true integration in a biorefinery will require appropriate separation technologies. Compared to other separation technologies, the low energy consumption, greater separation efficiency, reduced number of processing steps, and high quality of the final product are the main attractions of membrane separation processes in biorefining and bio-energy production.

3. (c)

(i)

Here we have

D = 3000 units, C_0 = ₹15 per order, C_h = ₹5 per unit per year

$$\therefore \quad \text{EOQ} \qquad Q^* = \sqrt{\frac{2C_0D}{C_h}} = \sqrt{\frac{2\times 15\times 3000}{5}}$$

$$Q^* = 134.164 \text{ units} \qquad \textbf{Ans.}$$

$$\text{Optimal number of orders, } n = \frac{D}{Q^*} = \frac{3000}{134.164} = 22.36 \qquad \textbf{Ans.}$$

(ii) We are given:

D = 3000 units; C_0 = 250 per production run, C_h = ₹5 per unit per year; P = 4800 units

$$\therefore \quad \text{EOQ}, \qquad Q_1^* = \sqrt{\frac{2C_0D}{C_h}} \times \sqrt{\frac{P}{P-D}}$$

$$Q_1^* = \sqrt{\frac{2\times 250\times 3000}{5}} \times \sqrt{\frac{4800}{4800-3000}}$$

$$Q_1^* = 894.427 \text{ units} \qquad \textbf{Ans.}$$

Average duration of the production run,

$$t = \frac{Q_1^*}{D} = \frac{894.427}{3000} = 0.298 \text{ year} \qquad \textbf{Ans.}$$

(iii) When item is purchased from outside

$$\text{T.C}_1 = DC + \frac{D}{Q^*}\times C_0 + \frac{Q^*}{2}\times C_h$$

$$= 3000\times 32 + \frac{3000}{134.164}\times 15 + \frac{134.164}{2}\times 5$$

$$= ₹96670.82/-$$

when item is produced internally,

$$C' = 0.80 \times 32 = ₹25.6/-$$

$$\therefore \qquad T.C_2 = DC' + \frac{D}{Q_1^*}\times C_0 + \frac{Q_1^*}{2}\times\frac{P-D}{P}\times C_h$$

$$= 3000\times 25.6 + \frac{3000}{894.427}\times 250 + \frac{894.427}{2}\times\frac{4800-3000}{4800}\times 5$$

$$\therefore \qquad T.C_2 = ₹78477.05/-$$

$\because$ $T.C_2 < T.C_1$, hence the company should manufacture the product internally.

4. (a) (i)

Factors Adversely Affecting Collector System's Efficiency

The following factors which adversely affect the efficiency of a collector system are: Shadow, Cosine loss, Dust etc.

1. Shadow factor :

When the angle of elevation of the sun is less than 15° (i.e. around sunrise and sunset), the shadows of some of the neighbouring collector panels fall on the collector's surface.

The shadow effect is reduced with the increase of sun's elevation angle.

The shadow factor is given as:

$$\text{Shadow factor} = \frac{\text{Collector's surface receiving light}}{\text{Total collector's surface}}$$

Its value is less than 0.1 when the angle of elevation of sun is less than 15° and 1 during noon when angle of sun's elevation angle is nearly 90°.

2. Cosine loss factor :

When the collector's surface receives the sun rays perpendicularly, maximum power collection is realised. If the angle between the perpendicular to collector's surface and the direction of sun ray is θ, the area of sun beam intercepted by the collector's surface is proportional to cos θ. Hence solar power collected in proportional to cos θ as shown in figure.

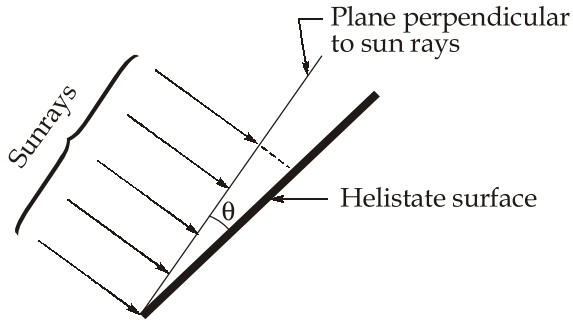

Exhibiting cosθ loss

- In case of fixed type collector panels cosine loss varies due to the daily variation and seasonal variation of the direction of sun rays.

3. Reflective loss factor :

The glass surface of the collector and the surface of the reflector collect dust, dirt and moisture. As a result, the reflector surface gets rusted, deformed and looses the shine. Hence, with the passage of time, the collector's efficiency is reduced significantly. Thus, to prevent the loss, daily maintenance, seasonal maintenance and yearly overhaul (change of seals, cleaning after dismantling) should be undertaken.

4. (a) (ii)

Given : $A_b = 2.5\ \text{km}^2 = 2.5 \times 10^6\ \text{m}^2$; $R = 12.5$ m; $r = 2.4$ m; $\eta_{gen} = 0.75$

Average power potential available $= 0.225 \times A_b \times (R^2 - r^2)$

$= 0.225 \times 2.5 \times 10^6 \times (12.5^2 - 2.4^2) \times 10^{-6}$

$= 84.65$ MW

$\therefore$ Average power generated $= 84.65 \times 0.75 = 63.49$ MW **Ans.**

Energy available in single emptying = $\frac{1}{2}\rho_{sw} \cdot A_b \cdot g \cdot \left(R^2 - r^2\right)$

$= \frac{1}{2} \times 1025 \times 2.5 \times 10^6 \times 9.8 \times \left(12.5^2 - 2.4^2\right)$

$= 1889590.06$ MJ

One ebb cycle duration = 12 h 25 min = 12.4167 h

Number of ebb cycles in a year = $365 \times \frac{24}{12.4167} = 705.5 \simeq 706$ cycle

Average annual energy generation = 1889590.06 × 706 × 0.75 J

$= 2.78 \times 10^8$ kWh

4. (b)

The network diagram for the given data is drawn in figure below:

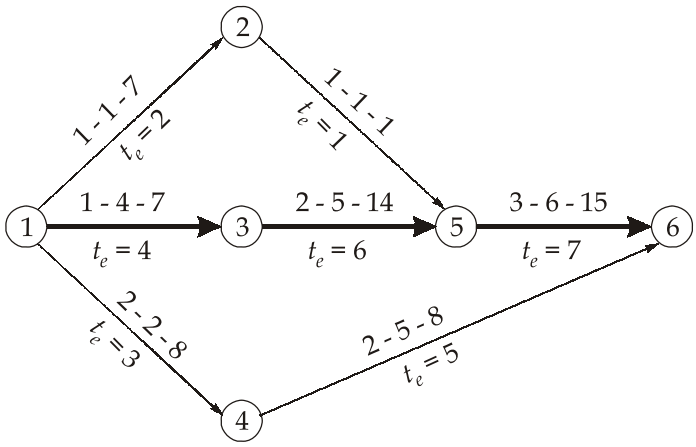

For determining the expected project length, the expected activity times need to be calculated. The same, along with the variances, are computed below.

Activity	t_0	t_m	t_p	$t_e = \frac{t_0 + 4t_m + t_p}{6}$	$\sigma^2 = \left(\frac{t_p - t_0}{6}\right)^2$
1 - 2	1	1	7	2	1
1 - 3	1	4	7	4	1
1 - 4	2	2	8	3	1
2 - 5	1	1	1	1	0
3 - 5	2	5	14	6	4
4 - 6	2	5	8	5	1
5 - 6	3	6	15	7	4

Since 1 - 3 - 5 - 6 has the longest duration, it is the critical path of the Network.

$\therefore$ $T_s = 17$ weeks **Ans. (i)**

Now, Variance, $\sigma^2 = 1 + 4 + 4 = 9$

$\therefore$ $\sigma = 3$ weeks

(ii) When the project due date is 18 weeks

$$\therefore \quad z = \frac{T_S - T_E}{\sigma} = \frac{18-17}{3} = 0.333$$

For which P = 0.6304 or 63.04%.

$\therefore$ The probability of meeting the due date is 63.04% and the probability of not meeting the due date is 36.96%. **Ans.**

(iii) If $T_s = 21$ weeks

$$\therefore \quad z = \frac{21-17}{3} = 1.333$$

For which, $P = 0.9087$ or 90.87% **Ans.**

The probability that the project will be completed on schedule is 90.87%.

4. (c) (i)

The power curve of a wind turbine indicates power output as a function of wind velocity at hub height as shown in figure. The curve shows the steady idealized characteristic, but in practice the wind speed constantly varies.

A wind turbine develops less power than the wind's stream power, due to friction and spillage and the curve in figure shows the following limiting speeds:

- **Cut-in speed (V_{in}):** It is the wind speed (14 km/h or 4 m/s) at which the turbine output begins. It is higher than the speed at which the turbine starts rotating. Before starting to rotate, the turbine remains in the braked position.

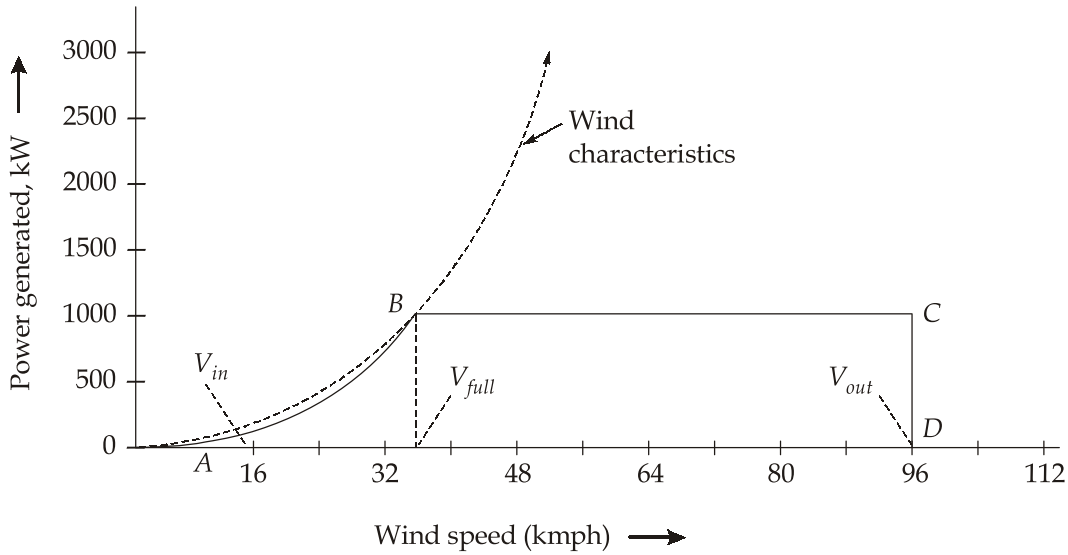

Wind turbine power curve

- **Rated speed (V_{full}):** It is the wind speed at which the turbine is designed to generate the rated power. When the wind speed is more than the 'cut-in speed' but less than the rated speed, the pitch angle of blades is selected to deliver maximum power. Pitch angle is controlled to maintain constant rated power above the rated wind speed.
- **Cut-out speed (V_{out}):** When the speed reaches the upper limit (90 kmph or 25 m/s) the turbine stops to generate power as a safety measure in order to protect the turbine and the generator.

As the wind reaches the cut-in speed V_{in} the WTG starts generating power; it then moves up to the point B to deliver the rated power. The blade pitch control operates at B to maintain a constant power output BC. At C, the cut-out wind speed is reached and the turbine is stopped to avoid structural damage.

The advantages with pitch regulation are:

- Pitch regulation makes it possible to rotate the blades to a position which stops and starts the rotor at any wind speed.
- With low wind speed, a pitch-regulated WEG can generate maximum torque to start the rotor.
- Pitch control system is not affected by change in air density and change in temperature due to placement of WEG at certain heights above sea level.
- It is easy to get a greater capacity factor for a pitch-regulated WEG.
- With pitch-regulated WEGs, the blades always experience laminar flow across the profile and turbulent, chaotic flow has no influence.

4. (c) (ii)

$$\text{Initially density of air, } \rho_1 = \frac{P_1}{RT_1} = \frac{101.325}{0.287 \times 293} = 1.205 \text{ kg/m}^3$$

Density of air at a height of 1900 mm,

$$\rho_2 = \frac{P_2}{RT_2} = \frac{0.86 \times 101.325}{0.287 \times 280} = 1.084 \text{ kg/m}^3$$

$$\text{Power generated, } P = \frac{1}{2}\rho A V_\infty^3$$

$$\frac{P_2}{P_1} = \frac{\rho_2 (V_\infty)_2^3}{\rho_2 (V_\infty)_1^3}$$

$$\Rightarrow \quad \frac{P_2}{1600} = \frac{1.084 \times \left(\frac{32 \times 1000}{3600}\right)^3}{1.205 \times \left(\frac{24 \times 1000}{3600}\right)^3}$$

$$\Rightarrow \quad P_2 = 3411.76 \text{ W}$$

$$\text{The change in output} = P_2 - P_1 = 3411.76 - 1600$$

$$= 1811.76 \text{ W}$$ **Ans.**

Section B

5. (a)

(i) Loose piece pattern

This type of pattern is used when the contour of the part is such that withdrawing the pattern from the mould is not possible. Hence, during moulding the obstructing part of the contour is held as a loose piece by a wire. After moulding is over, first the main pattern is removed and then the loose pieces are recovered through the gap generated by the main pattern as shown in figure below.

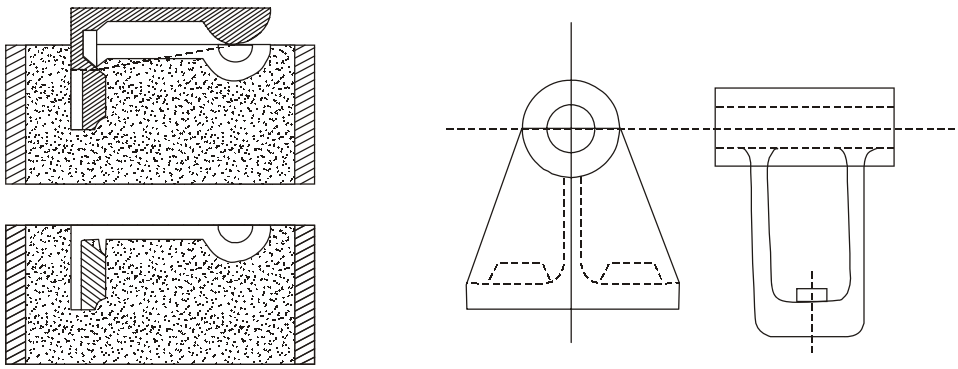

Losse piece pattern

Moulding with loose pieces is a highly skilled job and is generally expensive and therefore, should be avoided where possible.

(ii) Follow board pattern

This type of pattern is adopted for those castings where there are some portions which are structurally weak and if not supported properly are likely to break under the force of ramming. Hence the bottom board is modified as a follow board to closely fit the contour of the weak pattern and thus support it during the ramming of the drag. During the preparation of the cope, no follow board is necessary because the sand which is compacted in the drag will support the fragile pattern. An example is shown in figure below.

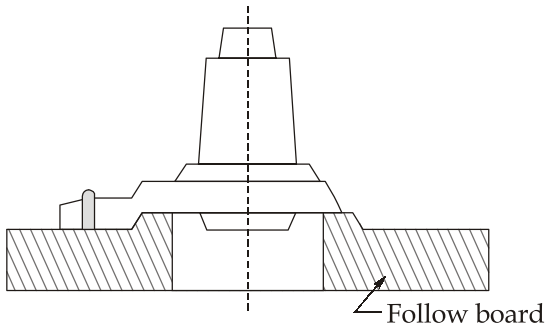

Follow board pattern

(iii) Sweep pattern

It is used to sweep the complete casting by means of a plane sweep. These are used for generating large shapes which are axi-symmetrical or prismatic in nature such as bell shaped or cylindrical as shown in figure below.

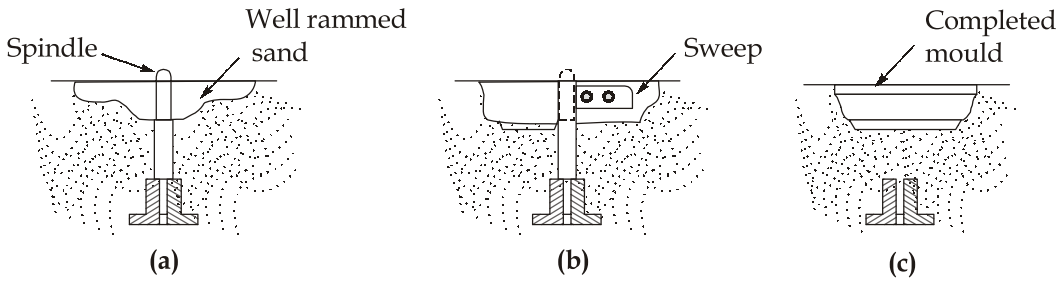

Sweep pattern

This greatly reduces the cost of a three dimensional pattern. This type of pattern is particularly suitable for very large castings such as the bells for ornamental purposes used which are generally cast in pit moulds.

5. (b)

Given : $M = 200$ kg; $r = \dfrac{0.580}{2} = 0.29$ m; $I_w = 1.25$ kgm^2; $I_e = 0.25$ kgm^2; $G = \dfrac{\omega_e}{\omega_w} = 5$;

$h = 0.54$ m; $R = 30$ m; $V = \dfrac{54 \times 1000}{3600} = 15$ m/s

$$\text{Gyroscopic couple, } C_G = (2I_w + 5I_e) \times \frac{V^2}{rR} \cos\theta$$

$$C_G = (2 \times 1.25 + 5 \times 0.25) \times \frac{15^2}{0.29 \times 30} \cos\theta = 96.98\cos\theta$$

$$\text{Centrifugal couple, } C_C = \frac{MV^2}{R} h\cos\theta$$

$$C_C = \frac{200 \times 15^2}{30} \times 0.54\cos\theta = 810\cos\theta$$

$$\text{Total overturning couple} = C_G + C_C = (96.98 + 810)\cos\theta = 906.98\cos\theta$$

$$\text{Righting couple} = Mgh\sin\theta = 200 \times 9.81 \times 0.54 \times \sin\theta$$

$$= 1059.48 \times \sin\theta$$

$$\therefore \quad 906.98 \times \cos\theta = 1059.48 \times \sin\theta$$

$$\Rightarrow \quad \tan\theta = \frac{906.98}{1059.48}$$

$$\Rightarrow \quad \theta = 40.56° \qquad \textbf{Ans.}$$

5. (c)

$$\text{Extrusion pressure, } \sigma_{x0} = \frac{\sigma_0(1+B)}{B}\left[1 - R^B\right]$$

Now, $$R = \left(\frac{r_0}{r_f}\right)^2 = \left(\frac{10}{4}\right)^2 = 6.25$$

$$B = \mu\cot\alpha = 0.1 \times \cot 45° = 0.1$$

$$\therefore \quad \sigma_{x0} = 250 \times \frac{1.1}{0.1}\left(1 - 6.25^{0.1}\right)$$

$$= 553.09 \text{ MPa} \qquad \text{(Compressive)}$$

Taking Tresca's condition, $k = \tau_1 = \dfrac{\sigma_0}{2} = \dfrac{250}{2} = 125$ MPa (Sticking friction)

$\therefore$ Taking extrusion pressure,

$$P_e = \sigma_{x_0} + \frac{4\tau_1 L}{D}$$

$$= 553.09 + \frac{4 \times 125 \times 37.5}{20} = 1490.6 \text{ MPa}$$

$\therefore$ Extrusion load $= P_e \times \pi r_0^2$

$= 1490.6 \times \pi \times 0.1^2 = 46.83$ MN **Ans.**

5. (d)

The law of gearing states that the common normal at the point of contact between a pair of teeth must always pass through the pitch point. Law of gearing is also called condition for constant velocity ratio i.e., the ratio of angular velocity of the two gears is equal to the reciprocal of the ratio of the distance between the centre of the gear and the pitch point of the two gears.

Let us consider the portions of the two teeth, one on the wheel 1 (or pinion) and the other on the wheel 2, as shown by thick line curves in figure below. Let the two teeth come in contact at point Q, and the wheels rotate in the directions as shown in the figure. Let T be the common tangent and MN be the common normal to the curves at the point of contact Q. From the centres O_1 and O_2, draw O_1M and O_2N perpendicular to MN. A little consideration will show that the point Q moves in the direction QC, when considered as a point on wheel 1, and in the direction QD when considered as a point on wheel 2.

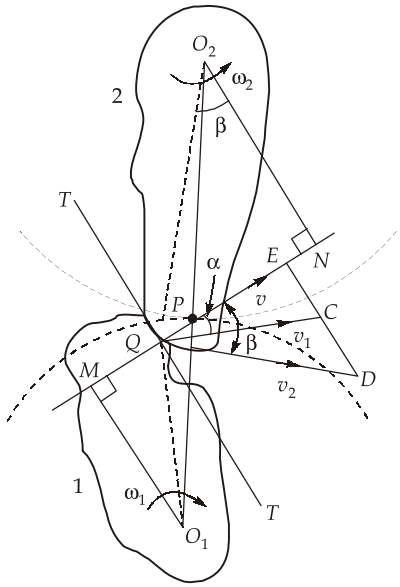

Let v_1 and v_2 be the velocities of the point Q on the wheels 1 and 2 respectively. If the teeth are to remain in contact, then the components of these velocities along the common normal MN must be equal.

$$\therefore \quad v_1 \cos\alpha = v_2 \cos\beta$$

or $$(\omega_1 \times O_1Q)\cos\alpha = (\omega_2 \times O_2Q)\cos\beta$$

$$(\omega_1 \times O_1Q)\frac{O_1M}{O_1Q} = (\omega_2 \times O_2Q)\frac{O_2N}{O_2Q}$$

or $$\omega_1 \times O_1M = \omega_2 \times O_2N$$

$$\therefore \quad \frac{\omega_1}{\omega_2} = \frac{O_2N}{O_1M} \qquad ...(i)$$

Also from similar triangles O_1MP and O_2NP,

$$\frac{O_2N}{O_1M} = \frac{O_2P}{O_1P} \qquad ...(ii)$$

Combining equations (i) and (ii), we have

$$\frac{\omega_1}{\omega_2} = \frac{O_2N}{O_1M} = \frac{O_2P}{O_1P} \qquad ...(iii)$$

From above, we see that the angular velocity ratio is inversely proportional to the ratio of the distances of the point P from the centres O_1 and O_2, or the common normal to the two surfaces at the point of contact Q intersects the line of centres at point P which divides the centre distance inversely as the ratio of angular velocities.

5. (e)

(i) **Open-loop system:** In the open-loop system, the signals are sent to the servomotor by the controller but the movements and final positions of the work table are not checked for accuracy. In this system the communication between the controller system and motor is one way. There is no feedback to the controller system. Open loop systems run the risk of overloading the machine and sometimes lacks accuracy.

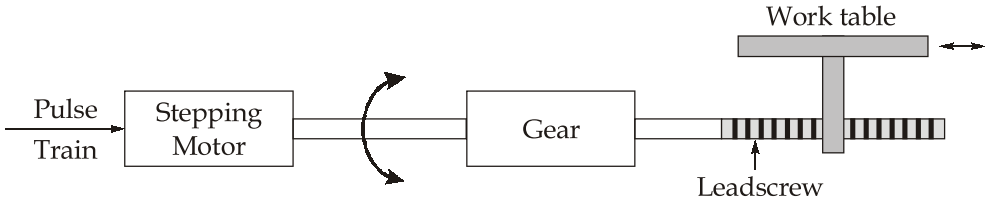

(ii) **Closed-loop system:** This system is equipped with various transducers, sensors and counters that measure accurately the position of the work table. Through feedback control, the position of the work table is compared against the signal. Table movements terminate when the proper coordinates are reached. The closed-loop system is more complicated and more expensive than the open-loop system.

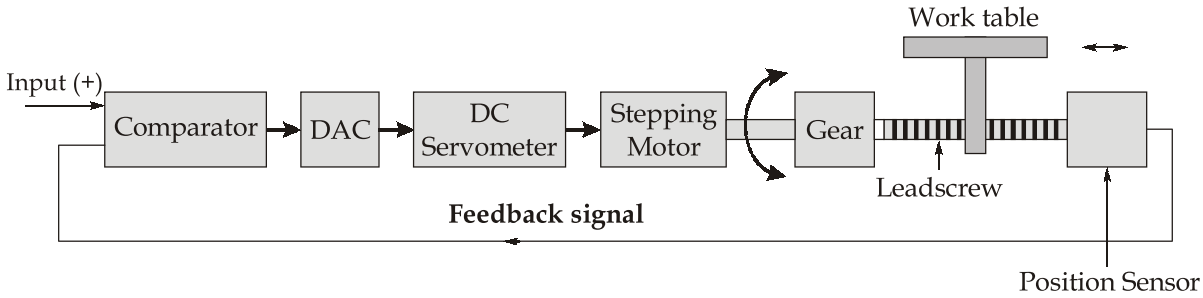

Feedback is not possible in open-loop control systems as it is in this system, the current state of output is not measured. So, no information is sent to the controller from the output of the system for comparison with the input signal.

Adaptive control systems: In adaptive control system, the operating parameters automatically adapt themselves to conform to new circumstances, such as changes in the dynamics of the particular process and any disturbance that may arise. This approach is basically a feedback system. The purpose of adaptive control are:

1. To optimize production rate
2. To optimize product quality
3. To minimize cost

In adaptive control, the system is capable of automatic adjustments during processing, through closed loop feedback control mechanism.

6. (a)

Given : m = 2500 kg; k = 400 mm = 0.4 m; N = 2820 rpm

$$I = mk^2 = 2500 \times 0.4^2 = 400 \text{ kgm}^2$$

$$\omega = \frac{2\pi N}{60} = \frac{2\pi \times 2820}{60} = 295.3 \text{ rad/s}$$

(i) When ship turns right at a radius of 220 m with a speed of 24 km/h

$$\omega_p = \frac{V}{R} = \frac{\left(\frac{24 \times 1000}{3600}\right)}{220} = 0.0303 \text{ rad/s}$$ **Ans.**

$$\therefore \quad c = I\omega\omega_p = 400 \times 295.3 \times 0.0303$$

$$= 3579.036 \text{ Nm}$$ **Ans.**

The effect of gyroscopic couple is to lower the bow and raise the aft.

(ii) Amplitude of swing, $\theta_0 = 6° = 6 \times \frac{\pi}{180°} = 0.1047$ rad

$$T = 42\text{s}$$

$$\text{Angular velocity, } \omega_0 = \frac{2\pi}{42} = 0.1496 \text{ rad/s}$$

$\therefore$ Maximum angular velocity of precession,

$$\omega_p = \theta_0 \cdot \omega_0$$

$$\omega_p = 0.1047 \times 0.1496 = 0.01566 \text{ rad/s}$$

$\therefore$ $$c = I\omega\omega_p = 400 \times 295.3 \times 0.01566$$

$$= 1849.76 \text{ Nm}$$

As bow descends during pitching, the ship would turn towards starboard.

(iii) $$\omega_p = 0.048$$

$$c = I\omega\omega_p = 400 \times 295.3 \times 0.048$$

$$= 5669.76 \text{ Nm}$$

As the axis of spin is always parallel to the axis of precession for all positions, there is no gyroscopic effect on the ship.

Maximum angular acceleration during pitching,

$$\alpha_{max} = \theta_0 \cdot \omega_0^2 = 0.1047 \times 0.1496^2$$

$$= 0.0023 \text{ rad/s}^2$$ **Ans.**

6. (b)

The properties and behaviour of dislocations are characterized by certain geometries, which are as follows:

1. A crystal normally consists of a large number of dislocations. Hence, there exist numerous Burger's vectors. The sum of these vectors meeting at a point called nodal point inside the crystal remains zero.
2. A dislocation does not abruptly end within the crystal. It vanishes either at the nodal point or on the surface of the crystal.
3. A dislocation under the influence field may close on as a loop. The profile of the loop may be circle or edge.
4. The distortional energy associated with dislocations may be the source of crystal's instability. The distortional energy is produced due to tensile and compressive stresses/strains field around the edge dislocation and due to shear stress-shear strain field in the case of screw dislocations.

5. The elastic strain energy is directly proportional to the square of the Burger's vector $\bar{b}$,

$$u = \frac{\pi}{8}Gb^2 \simeq \frac{Gb^2}{2}$$

where G is the shear modulus of the material.

6. The dislocations may have Burger's vectors of full lattice translation (a) or partial translation of a, i.e.

$$a, 2a, 3a, \text{ or } a/2, a/3, ...$$

7. The dislocations have inherent tendency to keep smallest possible Burger's vector, which enhances the stability of the crystal.

8. Two edge dislocations of opposite sign ⊥ and T and of equal Burger's vector and on the same slip plane cancel out each other. This is because the distortional strain energy fields superimpose and cancel each other.

9. The edge dislocation travels much faster (about 50 times) than the screw dislocations. The edge dislocations in a crystal are much more in number than the screw dislocations in any crystalline material.

10. Due to plastic deformation of the crystal, the dislocations get multiplied.

Dislocation Climb

A plane perpendicular to the glide plane is a climb plane and an edge dislocation can climb up or down. So, edge dislocations can go up or come down in the climb plane. The movement of atoms and vacancies at high temperature is the cause of this motion. A crystal contains an edge dislocation AB and a vacancy along the row at V [Figure (a)]. When the row of atoms at B shifts to vacancy site V, the extra plane AB of atoms shrinks due to subtraction of row of atoms at B. The edge dislocation climbs up as shown in Figure (b). In the climb down process, there is an increase in the row of atoms below edge dislocations, thereby vacancies are filled or formed as the case may be. Screw dislocation cannot climb up or climb down. The edge dislocation climb is a diffusion-controlled process.

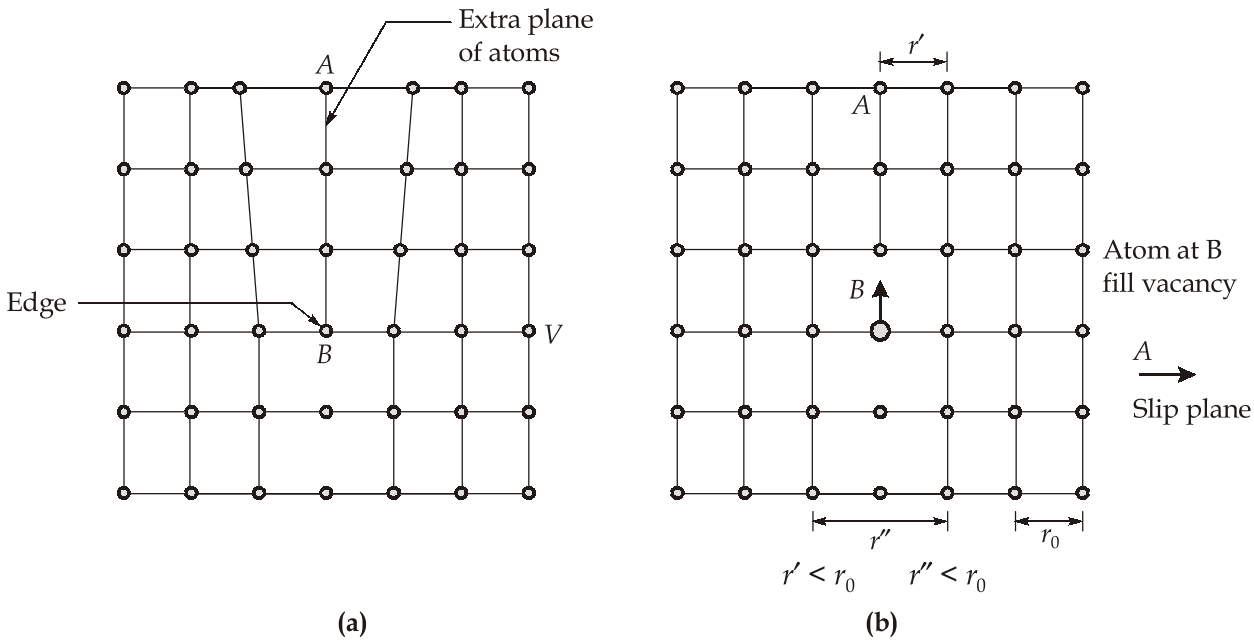

Figure (a) A crystal with Edge Dislocation *AB* and Vacancy at V (b) Vacancy at V is filled up

The positive climb causes the vacancies to annihilate while the negative climb generates vacancies. The climb motions require more energy than glide motions, because these are associated with migration of vacancies. Stress helps the climb motion. A compressive stress causes a positive climb and a tensile stress causes a negative climb.

The dislocation climb is necessary for polygonization and creep processes. Creep occurs due to diffusion of vacancies.

Cross Slip

A characteristic of FCC crystal lattice is that any Burger's vector is common to two slip planes. The screw dislocations have no fixed glide plane, and can surmount obstacles by gliding into another slip plane having a common slip direction. This is the process of cross slip.

A screw dislocation can gross slide or cross slip from one slip plane to another as shown in Figure (c). The screw dislocation first glides, then cross slips to a non-parallel plane $(1\,\bar{1}\,1)$. In the double cross slip process, it again cross slips back to (1 1 1) plane, which is parallel to the initial plane (Figure (c)). Cross slip is easier in metals with high stacking fault energy.

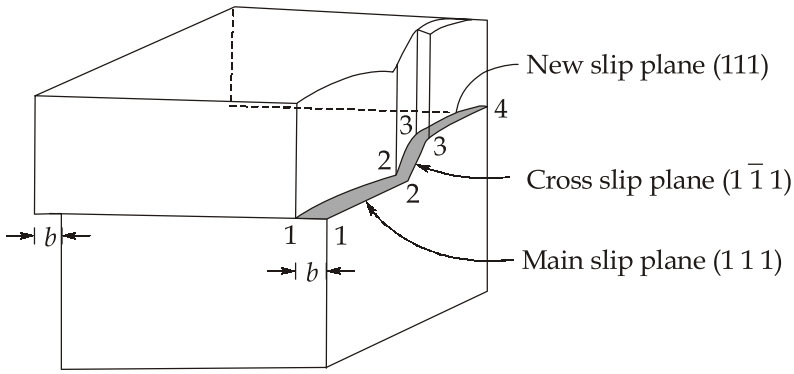

Cross-Slip

6. (c)

Given : r_c = 45 mm; N = 480 rpm; h = 25 mm; r_n = 10 mm; $\alpha = 80°$

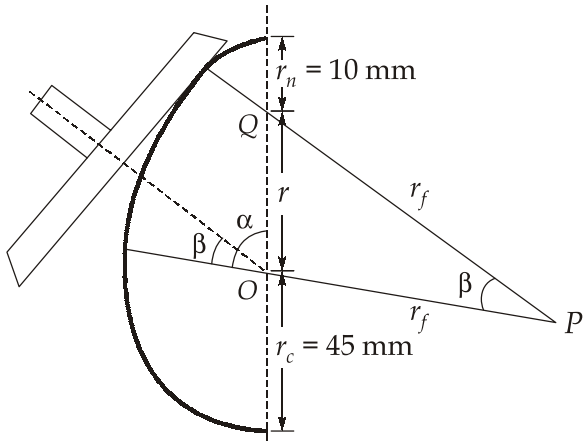

From the above figure,

$$r + r_n = r_c + h$$

$$\Rightarrow \quad r = r_c + h - r_n = 45 + 25 - 10 = 60 \text{ mm} \qquad \textbf{Ans.}$$

Also, $$(PQ)^2 = (OP)^2 + (OQ)^2 - 2 \times (OP) \times (OQ)\cos\angle POQ$$

$$\Rightarrow \quad (r_f - 10)^2 = (r_f - 45)^2 + 60^2 - 2 \times (r_f - 45) \times 60 \times \cos(180° - 80°)$$

$$\Rightarrow \quad r_f = 93.31 \text{ mm} \qquad \textbf{Ans.}$$

$$\therefore \quad OP = 93.31 - 45 = 48.31 \text{ mm}$$

$$PQ = 93.31 - 10 = 83.31 \text{ mm}$$

Applying sine rule of ΔDPQ, we have

$$\frac{OQ}{\sin\beta} = \frac{PQ}{\sin(180° - \alpha)}$$

$$\Rightarrow \quad \frac{r}{\sin\beta} = \frac{r_f - r_n}{\sin(180° - \alpha)}$$

$$\Rightarrow \quad \frac{60}{\sin\beta} = \frac{93.31 - 10}{\sin(180° - 80°)}$$

$$\Rightarrow \quad \beta = 45.17°$$

Acceleration when the follower is on the circular flank,

$$a = \omega^2 (r_f - r_c)\cos\beta$$

At the end of contact with the circular flank,

$$a = \left(\frac{2\pi \times 480}{60}\right)^2 \times \frac{(93.31 - 45)}{1000} \times \cos 45.17°$$

$$= 86.05 \text{ m/s}^2$$ **Ans.**

Acceleration when the follower is on the nose,

$$a = -\omega^2 r \cos(\alpha - \beta)$$

At the beginning of contact with the nose,

$$a = -\left(\frac{2\pi \times 480}{60}\right)^2 \times \frac{60}{1000} \times \cos(80° - 45.17°)$$

$$= -124.44 \text{ m/s}^2$$ **Ans.**

7. (a) (i)

Depending on the choke area there can be two types of gating systems:

- Non-pressurised gating system
- Pressurised gating system

A non-pressurised gating system having choke at the bottom of the sprue base, having total runner area and ingate areas higher than the sprue area. In this system there is no pressure existing in the metal flow system and thus it helps to reduce turbulence. This is particularly useful for casting drossy alloys such as aluminium and magnesium alloys. These have tapered sprues, sprue base wells and pouring basins. When the metal is to enter the mould cavity through multiple ingates, the cross section of the runner should accordingly be reduced at each of a runner break-up to allow for equal distribution of metal through all the ingates.

The gating ratio refers to the proportion of the cross-sectional areas between the sprue, runner and ingates and is generally denoted as sprue area: runner area: ingate area.

The gating ratio of a typical example is

Sprue : runner : ingate :: 1 : 4 : 4

The disadvantages of unpressurised gating are :

- The gating system needs to be carefully designed to see that all parts flow full. Otherwise some elements of the gating system may flow partially allowing for the air aspiration. Tapered sprues are invariably used with unpressurised system. Also the runners are maintained in drag while the gates are kept in cope to ensure that the runners are full.
- Casting yield gets reduced because of the large metal involved in the runners and gates.

In the case of a pressurised gating system normally the ingate area is the smallest, thus maintaining a back pressure throughout the gating system. Because of this back pressure in the gating system, the metal is more turbulent and generally flows full and thereby, can minimise the air aspiration even when a straight sprue is used (after the initial stages of pouring). When multiple gates are used, this system allows all the gates to flow full. These systems generally provide a higher casting yield since the volume of metal used up in the runners and gates is reduced. Because of the turbulence and the associated dross formation, this type of gating system is not used for light alloys but can be advantageously used for ferrous castings. Gating ratio of a typical pressurised gating system is

Sprue : runner : ingate :: 1 : 2 : 1

7. (a) (ii)

According to Chvorinov's rule,

$$\text{Solidification time, } t \propto \left(\frac{V}{A}\right)^2 \qquad \text{...(i)}$$

where, V and A are volume and surface area of the casting respectively.

From the expression (i), it is evident that for longer solidification time, the ratio $\left(\frac{V}{A}\right)$ should be maximum or the ratio $\left(\frac{A}{V}\right)$ should be minimum.

Now, $$V = \frac{\pi}{4}d^2 \times h,$$

where, d and h are the diameter and height of the cylinder respectively,

or, $$h = \frac{4V}{\pi d^2} \qquad \text{...(ii)}$$

Also, $$A = \pi d \times h + 2 \times \frac{\pi}{4} d^2$$

$$= \pi d \times \frac{4V}{\pi d^2} + \frac{\pi}{2} d^2 = \frac{4V}{d} + \frac{\pi}{2} d^2$$

For A to be minimum for a given V,

$$\frac{dA}{dd} = 0$$

i.e. $$\frac{d}{dd}\left(\frac{4V}{d} + \frac{\pi}{2} d^2\right) = 0$$

or, $$-\frac{4V}{d^2} + \pi d = 0 \text{ or } -4V + \pi d^3 = 0$$

or, $$d^3 = \frac{4V}{\pi}$$

Also, $$\frac{4V}{\pi} = hd^2$$ [from expression (ii)]

$\therefore$ $$d^3 = hd^2$$

or, $$d = h$$ **Proved.**

This optimum is true only for a side riser.

7. (b) (i)

Helix Angle (ψ) : It is the angle at which the teeth are inclined to the axis of a gear. It is also known as spiral angle.

Circular Pitch (p) : It is the distance between the corresponding points on adjacent teeth measured on the pitch circle. It is also known as transverse circular pitch.

Normal Circular Pitch (p_n): Normal circular pitch or simply normal pitch is the shortest distance measured along the normal to the helix between corresponding points on the adjacent teeth. The normal circular pitch of two mating gears must be same.

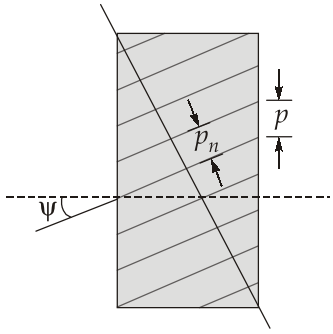

7. (b) (ii)

Given : $\theta = 70°$; $P_n = 14$ mm; $VR = 1.8$; $C = 160$ mm; $\phi = 6°$

Let ψ_1 be the spiral angle of the wheel 1

Then, the spiral angle of the wheel 2,

$$\psi_2 = 70° - \psi_1 \quad \text{...(i)}$$

Velocity ratio, $VR = 1.8$

$$VR = \frac{d_1 \cos\psi_1}{d_2 \cos\psi_2} = \frac{T_1}{T_2} = 1.8$$

$$\Rightarrow \quad T_1 = T_2 \times 1.8 \qquad \text{...(ii)}$$

Also, $$\frac{\cos\psi_1}{\cos\psi_2} = 1.8$$

$$\Rightarrow \quad \cos\psi_1 = 1.8\cos(70° - \psi_1) \qquad \text{[from equation (i)]}$$

$$\Rightarrow \quad \psi_1 = 12.80° \qquad \textbf{Ans.}$$

and $$\psi_2 = 70 - 12.80° = 57.20° \qquad \textbf{Ans.}$$

$$\text{Centre distance, } C = \frac{P_n}{2\pi}\left[\frac{T_1}{\cos\psi_1} + \frac{T_2}{\cos\psi_2}\right]$$

$$\Rightarrow \quad 160 = \frac{14}{2\pi}\left[\frac{T_2 \times 1.8}{\cos 12.80°} + \frac{T_2}{\cos 57.20°}\right] \qquad \text{[from equation (ii)]}$$

Solving above equation, we get

$$\Rightarrow \quad T_2 = 19.45 \simeq 20 \text{ (say)} \qquad \textbf{Ans.}$$

$$\Rightarrow \quad T_1 = 1.8 \times 20 = 36 \qquad \textbf{Ans.}$$

$$\therefore \quad C_{exact} = \frac{14}{2\pi}\left[\frac{36}{\cos 12.80°} + \frac{20}{\cos 57.20°}\right] = 164.52 \text{ mm} \qquad \textbf{Ans.}$$

$$\text{Efficiency, } \eta = \frac{\cos(\psi_2 + \phi)\cos\psi_1}{\cos(\psi_1 - \phi)\cos\psi_2}$$

$$= \frac{\cos(57.20° + 6°) \times \cos 12.80°}{\cos(12.80° - 6°)\cos 57.20°}$$

$$= 0.8174 \text{ or } 81.74\%$$

7. (c) (i)

Advantages of backward extrusion are as follows:

1. A 25 to 30% reduction in maximum force relative to direct extrusion takes place.
2. There is no relative displacement between the billet and container. Therefore, extrusion pressure is not a function of billet length. Hence billet length is not limited by the load required for this displacements.
3. Between billet and container no heat is produced by friction, so there will not be any temperature increase at the billet surface towards end of the extrusion. Therefore there is lesser tendency towards cracking of the surfaces and edges and extrusion speeds can be significantly higher.

4. The tool life is more in backward extrusion, because of reduced friction and temperatures.

7. (c) (ii)

Given : $h_i = 80$ mm; $D_i = 120$ mm; $h_f = h = 40$ mm; $\mu = 0.1$; $\sigma_0 = 120$ MPa

Now, Volume of cylinder before forging = Volume of cylinder after forging

$$\frac{\pi}{4}D_i^2 h_i = \frac{\pi}{4}\times D_f^2 \times h_f$$

$$\therefore \quad D_f^2 = D_i^2 \times \frac{h_i}{h_f}$$

$$\therefore \quad D_f = 120 \times \sqrt{\frac{80}{40}} = 169.705 \text{ mm}$$

or $\quad R_f = 84.852 \text{ mm} = R$

For sliding, $\quad P = 2ke^{\frac{2\mu}{h}(R-r)}$

where $\quad 2k = \sigma_0 = 120$ MPa

$$\therefore \quad P = 2ke^{\frac{2\times 0.1}{40}(84.852-r)}$$

So, forging load is given by

$$F = \int_0^R P\cdot 2\pi r dr$$

$$\therefore \quad F = 2\pi\times 120\int_0^{84.852} r\cdot e^{\left(\frac{84.852-r}{200}\right)}$$

$$= 240\pi\left[(-200)re^{\left(\frac{84.852-r}{200}\right)} - \int(-200)e^{\left(\frac{84.852-r}{200}\right)}\cdot dr\right]$$

$$= 240\pi\left[(-200)re^{\left(\frac{84.852-r}{200}\right)} - 200^2 e^{\left(\frac{84.852-r}{200}\right)}\right]_0^{84.852}$$

$$= 240\pi\left[\left(-200\times 84.852 - 200^2\right) - \left(0 - 200^2 e^{\left(\frac{84.852-r}{200}\right)}\right)\right]$$

$$F = 3.142 \text{ MN}$$

$\therefore$ Mean die pressure, $\overline{P} = \dfrac{F}{A_F} = \dfrac{3.142 \times 10^6}{\pi \times 84.852^2}$

$\overline{P} = 138.9$ MPa **Ans.**

8. (a) (i)

Ductile or Nodular Iron

Addition of a small amount of Magnesium and/or Cerium to the molten cast iron produces an entirely different microstructure with different mechanical properties. Magnesium removes any sulphur and oxygen present in the liquid melt. It is the residual magnesium that causes growth of spheroidal graphite. This inoculation provides different sites for graphite. In the microstructure, nodules or spherical particles of graphite appear, and the matrix phase surrounding these particles is pearlite (for moderate cooling) and ferrite (for slow cooling)-keeping the iron at 700°C for several hours as shown in figure (a).

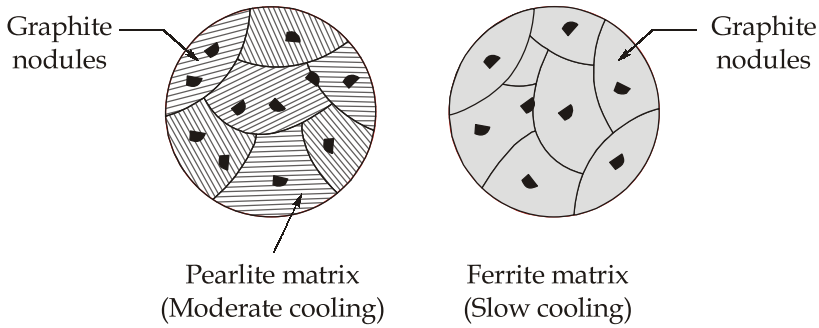

Figure (a) : Ductile Iron

Nodular cast irons are stronger and much more ductile than grey CI. Typical applications of nodular iron are valves, pump casings, crankshafts, gears and many automobile components.

Malleable Iron and White Cast Iron

For low silicon content (less than 1 per cent) in cast iron, on rapid cooling, most of the carbon exists as cementite. As a result, due to the presence of large amounts of cementite, white iron is extremely hard and brittle and difficult to machine. It has hard wear-resistant surface, and its use is limited in such applications as rollers in rolling mills subjected to high compressive stresses.

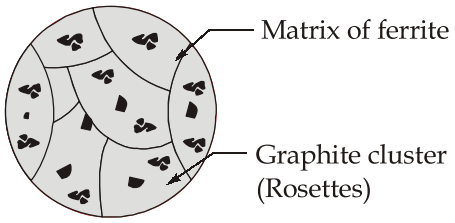

Figure (b) : Slow Cooling (Malleable Iron)

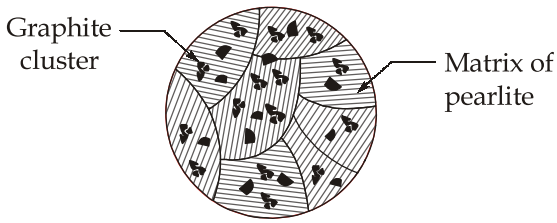

Figure (c) : Fast Cooling (Malleable Iron)

By a heat treatment process, white iron is converted into a malleable iron. Heating white iron at temperatures between 800°C and 900°C for prolonged time period, and in a neutral atmosphere (to prevent oxidation) causes decomposition of cementite forming graphite, which exists in the form of clusters or rosettes surrounded by ferrite matrix on slow cooling figure (b) and pearlite on fast cooling as shown in figure (c).

8. (a) (ii)

Let suffix 'f' and 'm' denote fibre and matrix respectively.

$$F_c = F_f + F_m = 50 \times 10^6 \times 300 \times 10^{-6}$$
$$= 15000 \text{ N}$$

Also $$\frac{F_f}{F_m} = \frac{\sigma_f A_f}{\sigma_m A_f}$$

Assuming that the strain on both the matrix and the fibre is equal,

$$\frac{F_f}{F_m} = \frac{E_f V_f}{E_m V_m} = \frac{70 \times 10^9 \times 0.4}{3.5 \times 10^9 \times 0.6}$$

$\therefore$ $$\frac{F_f}{F_m} = 13.33$$

or $$F_f = 13.33\, F_m$$

or $$F_m + 13.33 F_m = 15000$$

$\therefore$ $$F_m = \frac{15000}{14.33} = 1046.75 \text{ N}$$

and $$F_f = 13.33 \times 1046.75$$

$\therefore$ $$F_f = 13953.24 \text{ N}$$

The fibre supports the major portion of the applied load.

8. (b)

Given : m_B = 30 kg; m_C = 45 kg and m_D = 40 kg; r_A = 160 mm, r_B = 200 mm, r_C = 120 mm and r_D = 180 mm

Angular position with respect to *b* in counter clockwise direction (taking $\theta_B = 0°$), $\theta_C = 90°$, $\theta_D = 200°$

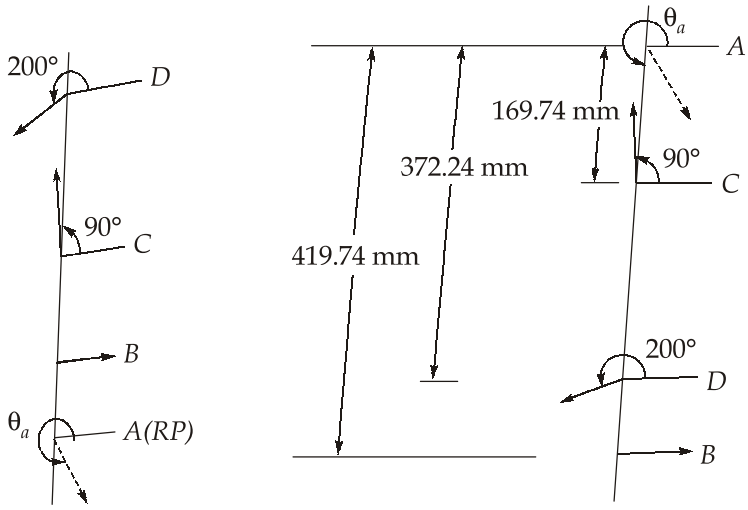

(a) **(b)**

Planes	Mass (kg)	Radius *r* (m)	*m*· *r* (kgm)
A(R.P.)	m_A	0.16	$0.16m_A$
B	30	0.2	6
C	45	0.12	5.4
D	40	0.18	7.2

$$\sum mr\cos\theta = 0$$

$$\Rightarrow \quad 0.16 \times m_A \cos\theta_A + 6 \times \cos 0° + 5.4 \times \cos 90° + 7.2 \times \cos 200° = 0$$

$$\Rightarrow \quad m_A \cos\theta_A = 4.7862 \qquad \text{...(i)}$$

Similarly, $\sum mr\sin\theta = 0$

$$\Rightarrow \quad 0.16 \times m_A \sin\theta_A + 6 \times \sin 0° + 5.4 \times \sin 90° + 7.2 \times \sin 200° = 0$$

$$\Rightarrow \quad m_A \sin\theta_A = -18.3591 \qquad \text{...(ii)}$$

Squaring and adding equation (i) and (ii), we get

$$m_A = 18.973 \text{ kg}$$ **Ans.**

Dividing (ii) by (i), we get

$$\tan\theta_A = \frac{-18.3591}{4.7862}$$

$$\Rightarrow \quad \theta_A = 284.61^\circ$$ **Ans.**

For complete balancing, couple equation are:

$$\sum mrl\cos\theta = 0$$

$$\Rightarrow \quad 6 \times l_b \times \cos 0^\circ + 5.4 \times l_c \times \cos 90^\circ + 7.2 \times l_d \times \cos 200^\circ = 0$$

$$\Rightarrow \quad l_b = 1.1276 \times l_d \quad \text{...(iii)}$$

$$\sum mrl\sin\theta = 0$$

$$\Rightarrow \quad 6 \times l_b \times \sin 0^\circ + 5.4 \times l_c \times \sin 90^\circ + 7.2 \times l_d \times \sin 200^\circ = 0$$

$$\Rightarrow \quad l_c = 0.456 \times l_d \quad \text{...(iv)}$$

$$\Rightarrow \quad l_b + 250 = 0.456 \times l_d$$

$$\Rightarrow \quad 1.1276 \times l_d + 250 = 0.456 \times l_d$$

$$\Rightarrow \quad l_d = -372.24 \text{ mm}$$

$$l_b = 1.1276 \times l_d = -419.74 \text{ mm}$$

$$l_c = l_b + 250 = -169.74 \text{ mm}$$

8. (c) (i)

Evaporative-pattern Casting (Lost foam)

This process is also known as lost-pattern casting and under the trade name "Full-mould process". It uses a polystyrene pattern, which evaporates upon contact with molten metal to form a cavity for the casting.

The evaporative-pattern casting process is carried out as follows:

- Raw expendable polystyrene (EPS) beads, containing 5% to 8% pentane (a volatile hydro- carbon), are placed in a preheated die, usually made of aluminium. The polystyrene expands and takes the shape of the die cavity. Additional heat is applied to fuse and bond the beads together.
- The die is then cooled and opened, and the polystyrene pattern is removed. Complex patterns may also be made by bonding various individual sections of the pattern, using hot-melt adhesive.
- The pattern is then coated with a water-base refractory slurry, dried, and placed in a flask.
- The flask is filled with loose fine sand, which surrounds and supports the pattern. The sand is periodically compacted by various means.
- Then, without removing the polystyrene pattern, the molten metal is poured into the mould. This action immediately vaporizes the pattern (an ablation process) and fills the mould cavity, completely replacing the space previously occupied by

the polystyrene pattern. The heat degrades (depolymerizes) the polystyrene, and the degradation products are vented into the surrounding sand.

Typical applications of this process are:

- Cylinder heads;
- Brake components and manifolds for automobiles;
- Crankshafts;
- Machine bases.

8. (c) (ii)

Drawing force on plug, $\sigma_d = \sigma_0 \frac{(1+B)}{B}\left[1-\left(\frac{h_1}{h_0}\right)^B\right]$

Here, $B = \frac{\mu_1+\mu_2}{\tan\alpha-\tan\beta}, \alpha = 15°, \beta = 0$

$\therefore \quad B = \frac{0.2}{\tan 15°} = 0.7464$

$\therefore \quad \frac{\sigma_d}{\sigma_0} = \frac{1.7464}{0.7464}\left[1-\left(\frac{1.25}{2}\right)^{0.7464}\right] = 0.692$

For movable mandrel, $\frac{\sigma_d}{\sigma_0} = \ln\left(\frac{1}{\frac{h_o}{h_1}-1}\right) = \ln\left(\frac{1}{\frac{2}{1.25}-1}\right)$

$\frac{\sigma_d}{\sigma_0} = 0.511$

$\therefore$ Use of movable mandrel substantially reduces the drawing force.